LS-77
W. Chou
January, 1987

VIBRATIONS OF THE MAGNET-PEDESTAL SYSTEM

This note provides an analysis of the vibrations of the magnet-pedestal system of the Argonne Advanced Photon Source. It consists of two parts and an appendix. Part I is a discussion of how to calculate the normal modes of the system. In Part II, the normal mode method is employed to study the response of the system to various kinds of excitations, in particular, to the ground motion. Some technical information is included in the appendix to make this note self-consistent. The dipole system is chosen to be an example to carry on explicit calculations and the main numerical results are summarized in Tables 1 and 2 and Figures 2 and 4.

Part I

Normal Modes of the Magnet-Pedestal System

A simplified model of the magnet-pedestal system of the Argonne Advanced Photon Source is a uniform girder supported by two elastic pedestals with stiffness k, see Fig. 1. This model can be used for an approximate calculation of the transverse vibration normal modes of the system. The method used in this part is similar to that of Ref. 1, but with different boundary conditions in solving the Euler equation. In the following, we give a brief description of this method.

The free transverse vibration of a uniform girder obeys the Euler equation

$$EI \frac{\partial^4 y}{\partial x^4} + \rho \frac{\partial^2 y}{\partial t^2} = 0 \ . \tag{1}$$

Let

$$y(x,t) = Y(x)\ e^{i2\pi ft}, \tag{2}$$

then (1) is reduced to an ordinary differential equation

$$\frac{d^4 Y}{dx^4} - \beta^4 Y = 0 \quad , \tag{3}$$

where

$$\beta = \left(\frac{\rho}{EI}\right)^{1/4} (2\pi f)^{1/2} \quad (\text{in}^{-1}) \quad ,$$

f = normal mode frequency of the system (Hz),
ρ = mass density of the girder (lb/in),
E = Young's modulus of the girder (lb/in^2),
I = moment of inertia of the girder (in^4).

The general solution to Eq. (3) is of the form

$$Y_i(x) = A_i \, ch\beta x + B_i \, sh\beta x + C_i \cos\beta x + D_i \sin\beta x, \tag{4}$$

where the subscript i indicates the solution of the i^{th} part of the girder (for instance, i = 1, 2, 3 in Fig. 1). The coefficients A, B, C and D are determined by the boundary conditions, which in our case can be described in the following way. The boundaries a and d in Fig. 1 are free ends. Therefore, both the moment and the shear force are zero, i.e.,

$$\begin{cases} Y'' = 0 \\ Y''' = 0 \end{cases} \qquad \text{for } x = x_a, \; x_d. \tag{5}$$

On boundary b, in addition to a zero moment, the sum of the shear and the elastic force should be zero, namely,

$$\begin{cases} Y_1'' = Y_2'' = 0 \\ EI(Y_1''' - Y_2''') - k \, Y_1 = 0 \\ Y_1 = Y_2 \end{cases} \qquad \text{for } x = x_b. \tag{6}$$

The same conditions apply to boundary c, with the subscripts 1 and 2 in Eq. (6) replaced by 2 and 3, respectively. Thus, we have altogether 12 boundary conditions associated with 12 unknown coefficients (A_i's, B_i's, etc.). The equations of the boundary conditions can be written in the vector form

$$\bar{\bar{H}} \, \bar{u} = 0 \; , \tag{7}$$

where

$$\bar{u} = \begin{pmatrix} A_1 \\ B_1 \\ \vdots \\ C_3 \\ D_3 \end{pmatrix} \tag{8}$$

is a 12-dimensional vector and $\bar{H}$ a 12×12 matrix derived from Eqs. (5) and (6). Following the method of Ref. 1 to simplify the calculation, one expresses A_i and C_i as the functions of B_i and D_i and, correspondingly, Eqs. (7) and (8) are reduced to

$$H\, u = 0, \tag{7'}$$

with

$$u = \begin{pmatrix} B_1 \\ D_1 \\ \vdots \\ B_3 \\ D_3 \end{pmatrix} \tag{8'}$$

a 6-dimensional vector and H a 6×6 matrix. In order to have non-zero solution u to (7'), we require that

$$\det H = 0 \quad . \tag{9}$$

The values of f, which satisfy (9), are then the normal frequencies of the system. The explicit form of H is given as follows:

$$H = \begin{pmatrix} 1 & -1 & 0 & 0 & & \\ -a_7^{(1)} & -a_8^{(1)} & a_1^{(2)} & a_2^{(2)} & 0 & \\ -a_3^{(1)} & a_4^{(1)} & a_5^{(2)} & -a_6^{(2)} & & \\ & & -a_7^{(2)} & -a_8^{(2)} & a_1^{(3)} & a_2^{(3)} \\ 0 & & -a_3^{(2)} & a_4^{(2)} & a_5^{(3)} & -a_6^{(3)} \\ & & 0 & 0 & a_7^{(3)} & a_8^{(3)} \end{pmatrix} \tag{10}$$

where

$$a_i^{(j)} = \frac{b_i^{(j)}}{\text{ch } \beta\ell_j - \cos \beta\ell_j} ,$$

$$b_1^{(j)} = -2 \text{ sh } \beta\ell_j + \alpha(\text{ch } \beta\ell_j - \cos \beta\ell_j) ,$$

$$b_2^{(j)} = 2 \sin \beta\ell_j - \alpha(\text{ch } \beta\ell_j - \cos \beta\ell_j) ,$$

$$b_3^{(j)} = \text{sh } \beta\ell_j \cdot \cos \beta\ell_j ,$$

$$b_4^{(j)} = \text{ch } \beta\ell_j \cdot \sin \beta\ell_j ,$$

$$b_5^{(j)} = \text{sh } \beta\ell_j ,$$

$$b_6^{(j)} = \sin \beta\ell_j ,$$

$$b_7^{(j)} = \alpha(1 - \text{ch } \beta\ell_j \cos \beta\ell_j - \text{sh } \beta\ell_j \cdot \sin \beta\ell_j) ,$$

$$b_8^{(j)} = \alpha(1 - \text{ch } \beta\ell_j \cos \beta\ell_j + \text{sh } \beta\ell_j \sin \beta\ell_j) ,$$

and $\alpha = \frac{EI}{k} \beta^3$ (dimensionless).

Eq. (9) can be solved numerically by invoking the subroutine DFACT of the CERN math library. Once the normal frequencies are known, the corresponding normal modes can be obtained by calling another subroutine, EISRG1, of the CERN library.

As an example, we calculate the first three modes of the dipole system of the GeV light source. The data used in the calculations are:

m (mass) = 9500 lb,
L (length) = 100 in,
E = 29×10^6 lb/in^2,
I = 2190 in^4,
k = 10×10^5 lb/in.

The results of the normal frequencies are listed in Table 1 below, and those of the normal modes (for ℓ_1 = 22.3 in) are shown in Fig. 2.

Table 1.

Normal Frequencies of the Dipole System

ℓ_1 (in)	1	10	20	22.3*	25
f_1 (Hz)	40.79	46.44	53.12	54.77	56.79
f_2 (Hz)	77.45	80.08	82.29	83.27	83.94
f_3 (Hz)	208.01	268.87	407.30	459.88	538.26

* when ℓ_1 = 0.223 L, the deflections at center and ends are the same.

The same method can be employed to calculate the normal modes of the girder supporting the combination of quadrupoles and sextupoles of the GeV light source.

Several conclusions can be drawn from our results: (i) The natural vibration frequencies of the system are adjustable (by changing ℓ_1) in a certain range. (ii) The first and the second harmonics are not too far away from each other ($f_2 < 2f_1$). This fact may be of concern because it might result in wide resonance bands. Fortunately, this does not happen in our case (see Part II). (iii) The two points of the girder where the pedestals are located give large deflections (see Fig. 2). Therefore, for a girder supporting several quadrupoles and sextupoles, one should (if possible) avoid these points when arranging the magnets. On the other hand, the "rest" points of the girder, R_1 and R_2 in Fig. 2, are insensitive to vibrations. Thus, one could put magnets there without much concern about their vibrations.

Part II

Response of the Magnet-pedestal System to the Ground Motion

The knowledge of the normal modes and frequencies of the magnet-pedestal system, which we have in Part I, is important in considering the response of the system to various kinds of excitations. This is due to the fact that the differential equations of motion are decoupled when the displacements are expressed in terms of the normal modes. This can be seen in the following way.

In the presence of the driving force, $F(x, t)$, and the damping force, $c \frac{\partial y}{\partial t}$, Eq. (1) is modified and takes the form

$$EI \frac{\partial^4 y}{\partial x^4} + c \frac{\partial y}{\partial t} + \rho \frac{\partial^2 y}{\partial t^2} = F(x,t), \tag{11}$$

in which c is the viscous damping per unit length and is assumed to be a constant (in unit lb • sec/in^2). (Another kind of damping, the structural damping, which is proportional to the internal elastic force, has been ignored.)

By using the normal mode method (see Ref. 2), we let the solution $y(x,t)$ of Eq. (11) be written as

$$y(x,t) = \sum_{s=1}^{n} Y^{(s)}(x)\, q^{(s)}(t). \tag{12}$$

where $Y^{(s)}(x)$ (dimensionless) is the s^{th} normal mode with normal frequency $\omega_s (\equiv 2\pi f_s)$ and $q^{(s)}(t)$ (unit in [in]) is to be determined through Eq. (11). Theoretically, the upper limit of the summation, n, should go to infinity, whereas practically, summation over first few modes will be, in general, good enough. Inserting the right-hand-side of Eq. (12) into Eq. (11) and interchanging the order of summation and differential, we get

$$\sum_{s=1}^{n} \left\{ EI \frac{d^4 Y^{(s)}}{dx^4} q^{(s)} + cY^{(s)} \frac{dq^{(s)}}{dt} + \rho\, Y^{(s)} \frac{d^2 q^{(s)}}{dt^2} \right\} = F(x,t). \tag{13}$$

Multiplying $Y^{(p)}$ and integrating over the whole length of the girder on both sides, Eq. (13) becomes

$$\sum_{s=1}^{n} \{ \int_a^d dx \, [EI \, Y^{(p)} \frac{d^4Y^{(s)}}{dx^4} q^{(s)} + cY^{(p)} \, Y^{(s)} \frac{dq^{(s)}}{dt} + \rho \, Y^{(p)}Y^{(s)} \frac{d^2q^{(s)}}{dt^2}]\}$$

$$= \int_a^d dx \, F(x,t) \, Y^{(p)}. \tag{14}$$

One can show that $Y^{(p)}$ and $Y^{(s)}$ are orthogonal to each other (see Appendix), namely

$$\int_a^d dx \, Y^{(p)}Y^{(s)} = \begin{cases} 0, & \text{if } s \neq p. \\ N_p, & \text{if } s = p. \end{cases} \tag{15}$$

In which N_p is the square of the normalization factor with unit [in]. In view of Eqs. (15) and (3), we have

$$\int_a^d dx \, EI \, Y^{(p)} \frac{d^4Y^{(s)}}{dx^4} = \begin{cases} 0 & , \text{ if } s \neq p. \\ \rho \, \omega_p^2 \, N_p, & \text{if } s = p. \end{cases} \tag{16}$$

It follows from Eq. (14) that

$$\rho \, \omega_p^2 \, q^{(p)} + c \frac{dq^{(p)}}{dt} + \rho \frac{d^2q^{(p)}}{dt^2} = \int_a^d dx \; F(x,t) \frac{Y^{(p)}}{N_p}. \tag{17}$$

Note that this differential equation for the p^{th} mode is decoupled from those for all other modes. This is actually the main advantage of this method. Eq. (17) is an ordinary differential equation for a forced-damped vibration of a system with just <u>one</u> degree of freedom, which can be solved by the standard method. (Recall that the original system is continuous and has infinitely many degrees of freedom!) Also note that in Eq. (17), $\rho\omega_p^2$ replaces the spring stiffness k in the conventional form of the vibration equation of one-degree-of-freedom system.

To solve Eq. (17), instead of considering a general driving force, we will content ourselves with the special case in which the driving force takes the form

$$F(x,t) = F_o \, e^{i\omega t} \, \delta(x-b) + F_o \, e^{i\omega t} \, \delta(x-c) \equiv F_b + F_c \, . \tag{18}$$

In other words, the driving force is harmonic with a magnitude F_o and a frequence ω; it affects the system only through the two pedestals at b and c. Furthermore, the phase difference between F_b and F_c is assumed to be zero for the current discussion. Plugging Eq. (18) into the right-hand side of Eq. (17), we get

$$\rho\omega_p^2\, q^{(p)} + c\,\frac{dq^{(p)}}{dt} + \rho\,\frac{d^2q^{(p)}}{dt^2} = F_o\left(\frac{Y^{(p)}(b) + Y^{(p)}(c)}{N_p}\right) e^{i\omega t} \tag{19}$$

in which $Y^{(p)}(b)$ and $Y^{(p)}(c)$ are the values of $Y^{(p)}(x)$ at points b and c, respectively. The solution to Eq. (19) can be written as

$$q^{(p)} = h^{(p)}\, e^{i(\omega t - \phi_p)} \ . \tag{20}$$

In this expression, the amplitude is expressed by

$$h^{(p)} = \frac{F_o\left(\frac{Y^{(p)}(b) + Y^{(p)}(c)}{N_p}\right) / (\rho\omega_p^2)}{\sqrt{\left[1 - \left(\frac{\omega}{\omega_p}\right)^2\right]^2 + \left(2\zeta_p \frac{\omega}{\omega_p}\right)^2}}, \tag{21}$$

where ζ_p is the damping factor:

$$\begin{aligned} \zeta_p &= \frac{c}{2\rho\omega_p} \\ &\equiv \frac{c}{(C_c)_p} \quad , \end{aligned} \tag{22}$$

in which the denominator $(C_c)_p = 2\rho\omega_p$ is the critical damping coefficient of the p^{th} mode. The phase, ϕ_p, in Eq. (20) has the following expression

$$\phi_p = \tan^{-1} \frac{2\zeta_p \frac{\omega}{\omega_p}}{1 - \left(\frac{\omega}{\omega_p}\right)^2} \ . \tag{23}$$

As we mentioned before, the term $\rho\omega_p^2$ in the numerator of the expression of

$h^{(p)}$, Eq. (21), is analogous to a spring with stiffness

$$k_p = \rho\omega_p^2 \quad . \tag{24}$$

(Recall that for a simple one-dimensional harmonic oscillator, one has $k = m\omega^2$.) The term

$$F_o\left(\frac{Y^{(p)}(b) + Y^{(p)}(c)}{N_p}\right) \equiv F^{(p)} \quad , \tag{25}$$

is the total strength of the driving force for the p^{th} mode. Therefore, one can define the dynamic amplification factor of the p^{th} mode, $M^{(p)}$, which is the ratio of the dynamic output to the static output, in the following way:

$$M^{(p)} = \frac{h^{(p)}}{F^{(p)}/k_p}$$

$$= \frac{1}{\sqrt{\left[1 - \left(\frac{\omega}{\omega_p}\right)^2\right]^2 + \left(2\zeta_p \frac{\omega}{\omega_p}\right)^2}} \tag{26}$$

The plot of $M^{(p)}$ and ϕ_p is shown in Fig. 3. The resonance occurs at

$$\omega_p^* = \omega_p \sqrt{1-2\zeta_p^2}$$

$$\approx \omega_p \text{ (for small } \zeta_p) \quad , \tag{27}$$

with the maximum value of $M^{(p)}$

$$M_{max}^{(p)} = \frac{1}{2\zeta_p \sqrt{1-\zeta_p^2}}$$

$$\approx \frac{1}{2\zeta_p} \text{ (for small } \zeta_p). \tag{28}$$

Another quantity, which may be of even more interest to us, is the transmissibility T. Because the driving force in our case is most likely induced by the ground motion, one can express the force directly in terms of the displacement $Ze^{i\omega t}$, of the ground motion. Here again, we assume that the ground motion at location b and c has the same amplitude, frequency and phase in order to simplify the calculations below. The equivalent magnitude of the force due to the ground motion is

$$F_o = kZ, \tag{29}$$

in which k is the stiffness of the pedestals. The amplitude of $q^{(p)}$ now takes the form

$$h^{(p)} = \frac{Z \cdot \frac{k}{\rho\omega_p^2}\left(\frac{Y^{(p)}(b) + Y^{(p)}(c)}{N_p}\right)}{\sqrt{\left[1 - \left(\frac{\omega}{\omega_p}\right)^2\right]^2 + \left(2\zeta_p \frac{\omega}{\omega_p}\right)^2}} . \tag{30}$$

The transmissibility, which is the ratio of the dynamic output to the dynamic input, can then be expressed as (for the p^{th} mode)

$$T^{(p)} = \frac{h^{(p)}}{Z}$$

$$= \frac{k}{\rho\omega_p^2}\left(\frac{Y^{(p)}(b) + Y^{(p)}(c)}{N_p}\right) \times \frac{1}{\sqrt{\left[1-\left(\frac{\omega}{\omega_p}\right)^2\right]^2 + \left(2\zeta_p \frac{\omega}{\omega_p}\right)^2}}$$

$$= \frac{k}{\rho\omega_p^2}\left(\frac{Y^{(p)}(b) + Y^{(p)}(c)}{N_p}\right) \times M^{(p)} \quad . \tag{31}$$

The plot of $T^{(p)}$ as a function of $\left(\frac{\omega}{\omega_p}\right)$ and ζ_p is similar to that of $M^{(p)}$ in Fig. 3.

In view of Eqs. (12), (20), (23), (30) and (31), the solution to Eq. (11) can be written as

$$y(x,t) = \sum_{p=1}^{n} Y^{(p)}(x)\, h^{(p)}\, e^{i(\omega t-\phi_p)}$$

$$= \sum_{p=1}^{n} Y^{(p)}(x)\, T^{(p)}_Z\, e^{i(\omega t-\phi_p)} \quad . \tag{32}$$

As an example of applications of this method, we consider again the dipole system of the GeV light source with the parameters given in Part I. Assume that $\ell_1 = 22.3$ inches. The first three normal frequencies are listed in Table 1. Note that $f_3 >> f_1$. The second mode (denoted by II in Fig. 2) is asymmetric which leads to the cancellation of $Y^{(2)}(b)$ by $Y^{(2)}(c)$. The associated transmissibility, $T^{(2)}$, is thus equal to zero. This is understandable because no asymmetric modes would be driven by the (currently assumed) symmetric driving force. It follows that the approximate solution to Eq. (11) can be expressed by a sum of just two terms:

$$y(x,t) \approx \left[Y^{(1)}(x)\, T^{(1)}\, e^{-i\phi_1} + Y^{(3)}(x)\, T^{(3)}\, e^{-i\phi_3}\right] Z e^{i\omega t} \quad . \tag{33}$$

We now consider five different cases:

(i) Low frequency region: $\omega < \omega_1 < \omega_3$.

In this case, we have

$$M^{(1)} \approx M^{(3)} \approx 1 \ ,$$

$$\phi_1 \approx \phi_3 \approx 0,$$

$$T^{(1)} = \frac{k}{\rho\omega_1^2}\left(\frac{Y^{(1)}(b) + Y^{(1)}(c)}{N_1}\right) M^{(1)}$$

$$\approx 2.3 \times 10^{-3},$$

$$T^{(3)} = \frac{k}{\rho\omega_3^2}\left(\frac{Y^{(3)}(b) + Y^{(3)}(c)}{N_3}\right) M^{(3)}$$

$$\approx 0.2 \times 10^{-3} ,$$

and

$$y(x,t) \approx \left(2.3 \times 10^{-3} \times Y^{(1)} + 0.2 \times 10^{-3} \times Y^{(3)}(x)\right) \times Z\, e^{i\omega t} .$$

The maximum amplitude occurs at the supporting points b and c and has the value

$$y_{max}(t) = (2.4 \times 10^{-3} + 0.08 \times 10^{-3}) \times Z\, e^{i\omega t}. \qquad (34)$$

It is apparent that the first mode is dominant in the low-frequency region.

(ii) Resonance at the 1st normal frequency: $\omega = \omega_1 < \omega_3$.

Assume that the damping factor

$$\zeta_1 = 0.005 , \qquad (35)$$

then one has

$$M^{(1)} = \frac{1}{2\zeta_1\sqrt{1-\zeta_1^2}} = 100 ,$$

$$M^{(3)} = 1,$$

$$\phi_1 = \frac{\pi}{2} ,$$

$$\phi_3 = 0 ,$$

$$T^{(1)} \approx 0.23 ,$$

$$T^{(3)} = \text{(negligible)} ,$$

and

$$y(x,t) \approx 0.23 \times Y^{(1)}(x) \times Z \times e^{i(\omega t - \frac{\pi}{2})} .$$

The maximum amplitude occurs in the middle point and has the value

$$y_{max}(t) = 0.26\ Z\ e^{i(\omega t - \frac{\pi}{2})} . \tag{36}$$

(iii) High frequency region: $\omega_1 < \omega < \omega_3$.

In this case,

$$M^{(1)} \approx 0 \ ,$$

$$M^{(3)} = 1 \ ,$$

$$\phi_1 = \pi \ ,$$

$$\phi_3 = 0 \ ,$$

$$T^{(1)} = 0 \ ,$$

$$T^{(3)} = 0.2 \times 10^{-3},$$

and

$$y(x,t) = 0.2 \times 10^{-3} \times Y^{(3)}(x) \times Z\ e^{i\omega t} .$$

The maximum amplitude which occurs at points b and c is

$$y_{max}(t) = 0.8 \times 10^{-4} \times Z\ e^{i\omega t}. \tag{37}$$

(iv) Resonance at the 3rd normal frequency: $\omega_1 < \omega = \omega_3$.

Assume the same damping factor as in (ii)

$$\zeta_3 = 0.005. \tag{38}$$

We get

$$M^{(1)} = 0 \quad ,$$

$$M^{(3)} = \frac{1}{2\zeta_3\sqrt{1-\zeta_3^2}} = 100 \quad ,$$

$$\phi_1 = \pi \quad ,$$

$$\phi_3 = \frac{\pi}{2} \quad ,$$

$$T^{(1)} = 0 \quad ,$$

$$T^{(3)} = 0.02 \quad ,$$

and

$$y(x,t) = 0.02 \times Y^{(3)}(x) \times Z\, e^{i(\omega t - \frac{\pi}{2})} \quad .$$

The maximum amplitude occurs at the supporting points b and c. Its value is

$$y_{max}(t) = 0.8 \times 10^{-2}\, Z\, e^{i(\omega t - \frac{\pi}{2})} \quad . \tag{39}$$

(v) Very high frequency region: $\omega_1 < \omega_3 < \omega$.

In this case, our assumption that there is no phase difference between the forces F_b and F_c is no longer valid. (The ground wave propagation velocity is about 2500 m/sec. At a frequency of 500 Hz, the wavelength is 5 m. Thus the distance between b and c is about 1/4 of the ground wave length.) Nevertheless, this should not be of concern because both $T^{(1)}$ and $T^{(3)}$ virtually vanish at this frequency region anyway.

From the above results, one can get the ratio y_{max}/Z, which we will call the vibration magnification factor. The results are summarized in Table 2 and are shown in Fig. 4.

Table 2

The vibration magnification factor of the dipole system

Driving frequency ($f = \omega/2\pi$)	$f < f_1$	$f = f_1$ ††	$f_1 < f < f_3$	$f = f_3$ ††	$f > f_3$
$\frac{y_{max}}{Z}$ †	0.25×10^{-2}	0.26	0.8×10^{-4}	0.8×10^{-2}	0

† y_{max} and Z are the vibration amplitudes of the girder and of the ground motion, respectively. The damping factor ζ is assumed to be 0.005 in the calculations (this is a relatively small value and is equal to the damping factor of the steel spring).

†† $f_1 = 54.77$ Hz and $f_3 = 459.88$ Hz for $\ell_1 = 22.3$ inches (see Table 1).

Discussions:

a. The vibration magnification factor is surprisingly small in all the cases above. Even at the first resonance with a quite small damping factor ($\zeta = 0.005$ is that of the steel spring) the magnification factor is still less than 1. This is basically due to the fact that the ratio of the stiffness of the pedestals to the equivalent stiffness of the girder [see Eq. (24)], $k/\rho\omega_p^2$, is very small (less than 10^{-3} in our case). Thus the driving force caused by the ground motion is significantly reduced when it is transmitted to the girder.

b. The second normal mode, which is asymmetric, might become important if the phase difference between F_b and F_c is close to π. However, this would require a driving frequency close to 1000 Hz, which is far beyond the second resonant frequency f_2 (83.27 Hz). Therefore, the second mode contributes nothing in any case.

Appendix

This appendix gives a proof that the eigenfunctions (the normal modes) of Eq. (3) with boundary condition (5) form an orthogonal set.

Let $Y^{(s)}$, $Y^{(p)}$ be two eigenfunctions of Eq. (3). The corresponding eigenvalues are $\lambda_s \equiv \beta_s{}^4$ and $\lambda_p \equiv \beta_p{}^4$, respectively.

$$Y^{(s)\prime\prime\prime\prime} = \lambda_s Y^{(s)} \quad , \tag{A1}$$

$$Y^{(p)\prime\prime\prime\prime} = \lambda_p Y^{(p)} \quad , \tag{A2}$$

where the apostrophe represents the differential with respect to x, $\frac{d}{dx}$. Multiplying both sides of (A1) and (A2) by $Y^{(p)}$ and $Y^{(s)}$, respectively, then subtracting (A2) from (A1) and integrating from boundary a to d, we get

$$\int_a^d \left[Y^{(p)}\, Y^{(s)\prime\prime\prime\prime} - Y^{(s)}\, Y^{(p)\prime\prime\prime\prime}\right] dx = (\lambda_s - \lambda_p) \int_a^d Y^{(s)} Y^{(p)} dx \ . \tag{A3}$$

We now evaluate the left-hand side of Eq. (A3) by integration by parts:

$$\int_a^d \left[Y^{(p)}\, Y^{(s)\prime\prime\prime\prime} - Y^{(s)}\, Y^{(p)\prime\prime\prime\prime}\right] dx$$

$$= \left[Y^{(p)}\, Y^{(s)\prime\prime\prime} - Y^{(s)}\, Y^{(p)\prime\prime\prime}\right] \Big|_a^d - \int_a^d \left[Y^{(p)\prime}\, Y^{(s)\prime\prime\prime} - Y^{(s)\prime}\, Y^{(p)\prime\prime\prime}\right] dx$$

$$= \left[Y^{(p)}\, Y^{(s)\prime\prime\prime} - Y^{(s)}\, Y^{(p)\prime\prime\prime}\right] \Big|_a^d - \left[Y^{(p)\prime} Y^{(s)\prime\prime} - Y^{(s)\prime}\, Y^{(p)\prime\prime}\right] \Big|_a^d$$

$$+ \int_a^d \left[Y^{(p)\prime\prime}\, Y^{(s)\prime\prime} - Y^{(s)\prime\prime}\, Y^{(p)\prime\prime}\right] dx \ .$$

The last term vanishes. The first two terms also vanish due to the boundary

condition (5). Therefore, the left-hand side of (A4) is zero. It follows that the right-hand side of (A4) should also be zero, namely,

$$(\lambda_s - \lambda_p) \int_a^d Y^{(s)} Y^{(p)} dx = 0 \ . \tag{A5}$$

If $\lambda_s \neq \lambda_p$, then one has

$$\int_a^d Y^{(s)} Y^{(p)} dx = 0 \ . \tag{A6}$$

In other words, the eigenfunctions of Eq. (3) with different eigenvalues are orthogonal to each other. This completes our proof.

The normalization of eigenfunctions in our case is not important. Because of some dimensional considerations, we would rather leave (the square of) the normalization factor

$$N_p = \int_a^d Y^{(p)} Y^{(p)} dx$$

explicitly in the equations in Part II. Note that N_p has the dimension of length [inch].

References

1. W. T. Weng and A. W. Chao, IEEE Trans. Nucl. Sci. NS-32, 3663 (1985).

2. W. C. Hurty and M. F. Rubinstein, Dynamics of Structures (Prentice-Hall, 1964), Chap. 8.

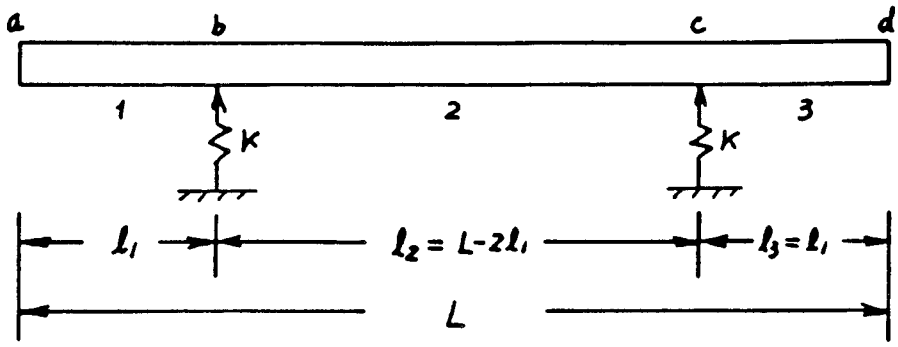

Fig. 1. A model of the magnet-pedestal system.

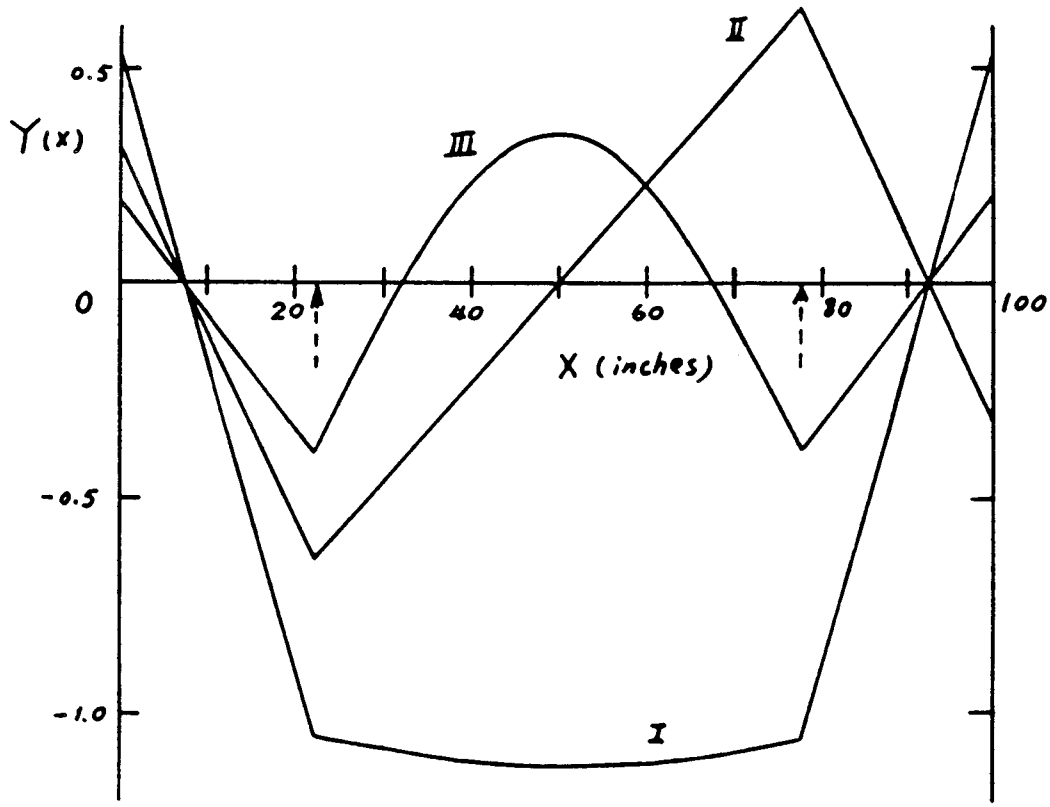

Fig. 2. The first three normal modes (I, II and III) of the dipole system. The two dashed arrows indicate the locations of the pedestals (x = 22.3 in and 77.7 in, resp.). R1 and R2 are the "rest" points. The deflection Y is in arbitrary unit.

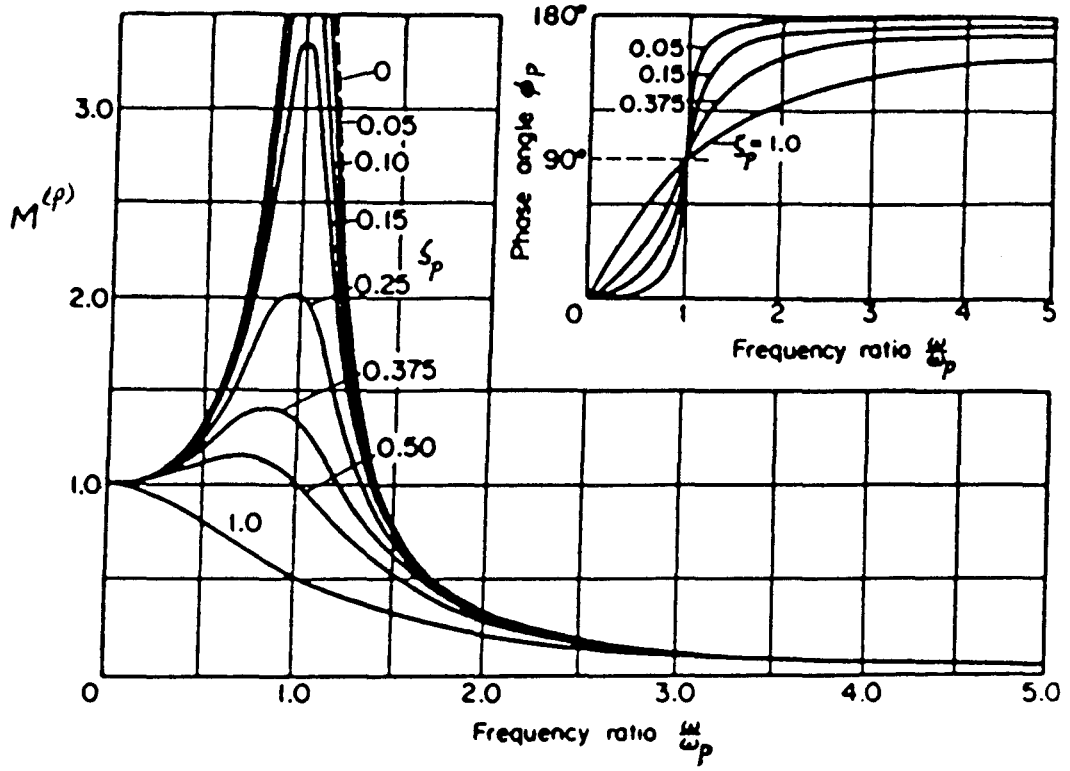

Fig. 3. The dynamic amplification factor M and the phase angle ϕ, see Eqs. (23) and (26).

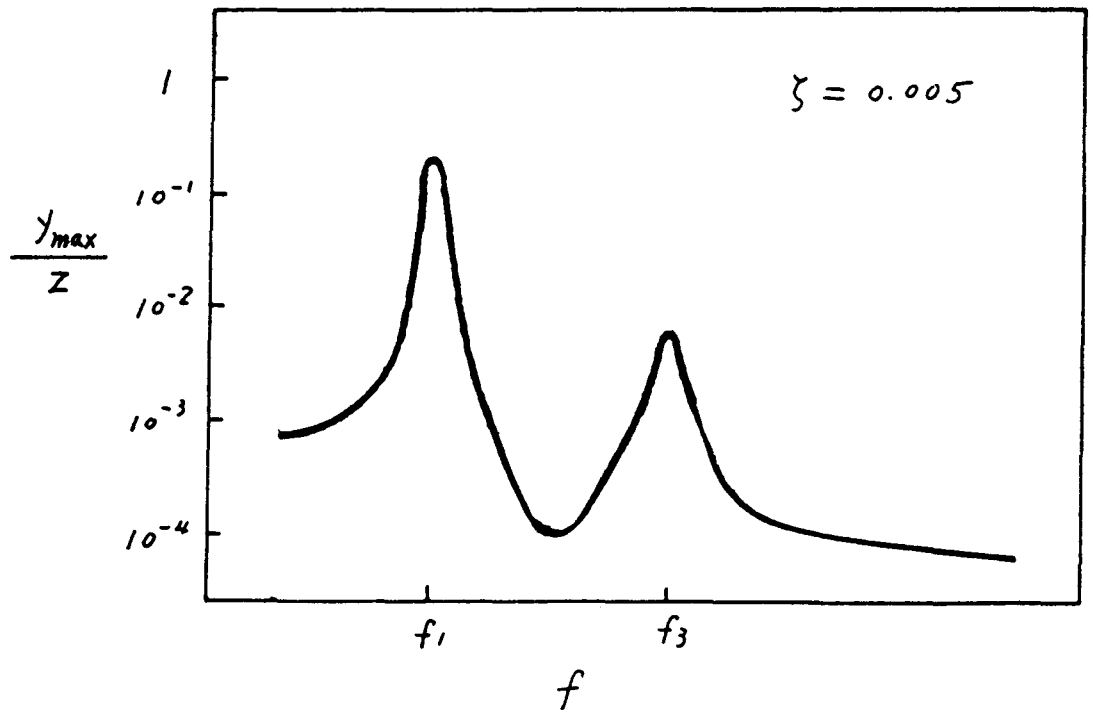

Fig. 4. The vibration magnification factor of the dipole system as a function of the ground vibration frequency. See Table 2. Here y_{max} and Z are the vibration amplitudes of the girder and of the ground motion, respectively; f_1 and f_3 are the first and third normal frequencies of the dipole system.

LS-77A(3/24/87)

Addendum to Note LS-77

1. After consulting some vibration experts,[1] the boundary conditions (6) in LS-77 are modified.

$$\begin{cases} Y_1' = Y_2' \\ Y_1'' = Y_2'' \\ EI(Y_1''' - Y_1''') - kY_1 = 0 \\ Y_1 = Y_2 \end{cases} \qquad \text{for } x = x_b. \qquad (6')$$

The same change applies for $x = x_c$. The form of the matrix H, Eq. (10), is altered accordingly. By using the method described in LS-77 and the new boundary conditions (6'), we recalculate the natural frequencies and the normal modes of the dipole system of the APS. The results are given in Table 1' and Fig. 2'.

2. The values of the vibration magnification factor, y_{max}/Z in Table 2 and Fig. 4, should be multiplied by 386.1, the gravitation acceleration constant. As a result, the part (a) of the discussion on page 16 of LS-77 is no longer valid. Using the data of Table 1' and Fig. 2', the values of y_{max}/Z are shown in Table 2' and Fig. 4'. The third mode with a frequency f_3 has no effects on the vibration magnification factor because of the zero values of the mode at the supporting points. The asymmetric first and fourth modes may contribute additional peaks in Fig. 4' if the phase difference between the ground vibrations at two supporting points are not negligible.

Reference

[1] M. Wambsganss and S. S. Chen, private communication.

Table 1'

The Natural Frequencies of the Dipole System

ℓ_1* (in)	1	10	22.3	25
f_1 (Hz)	40.6	43.7	43.3	39.1
f_2 (Hz)	75.8	62.8	45.3	45.2
f_3 (Hz)	201.4	187.8	180.9	181.1
f_4 (Hz)	505.8	499.1	500.7	501.5
f_5 (Hz)	981.0	977.6	979.5	979.2

*ℓ_1 is the distance between the ends and the supporting points (see Fig. 1 in LS-77). When ℓ_1 is equal to 0.223 times the length of the girder, the deflection at center and ends are the same.

Table 2'

The Vibration Magnification Factor of the Dipole System

Driving frequency	$f<f_2$	$f\sim f_2$††	$f_2<f<f_5$	$f\sim f_5$††	$f>f_5$
$\frac{y_{max}}{Z}$†	~1	1st peak	~0	2nd peak	→0

†y_{max} and Z are the vibration amplitudes of the girder and of the ground, respectively.

††f_2 = 45.3 Hz and f_5 = 979.5 Hz for ℓ_1 = 22.3 in (see Table 1').

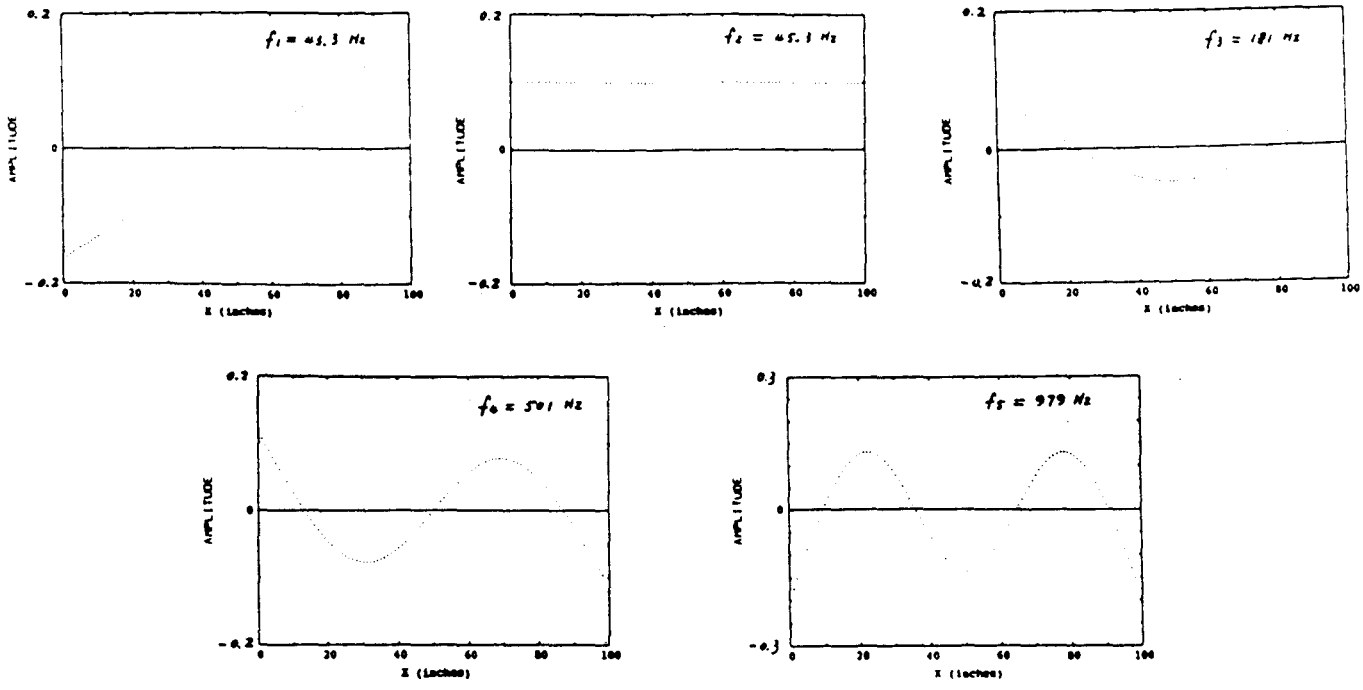

Fig. 2'. The first five normal modes of the dipole system of the APS (ℓ_1 = 22.3 in), when the boundary conditions (6') are applied. The first and the second mode are apparently close to that of a rigid body system.

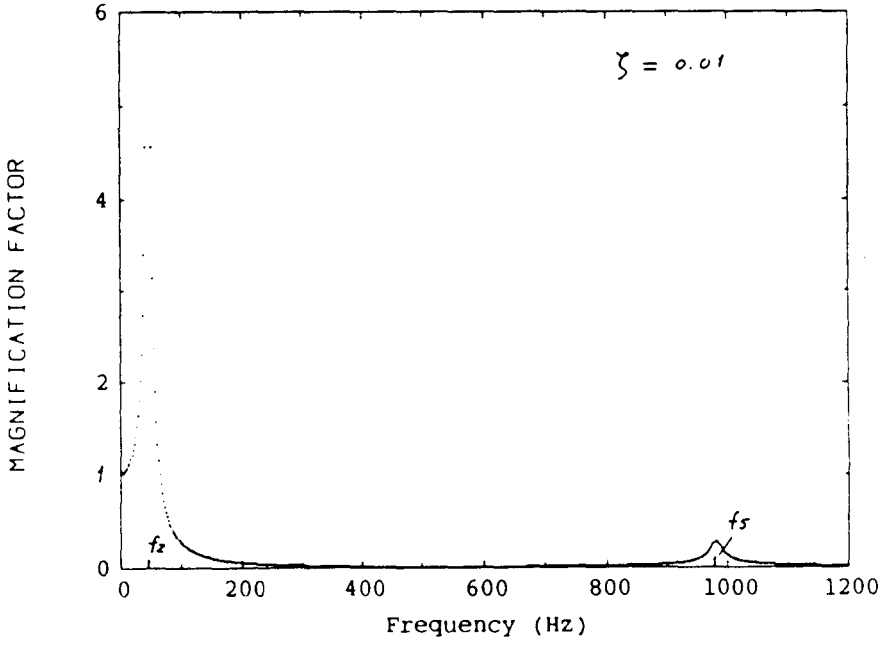

Fig. 4'. The vibration magnification factor, y_{max}/Z, of the dipole system of the APS.